RESEARCH PAPER

Synthesis and Characterization of Novel Hybrid Nanocomposite containing Modified Titanium Dioxide Nanoparticles with Copper and Phthalocyanine Pigment

Mehrnaz Gharagozlou[1*], Saeed Zhahabi[2]

[1] Department of Nanomaterials and Nanocoatings, Institute for Color Science and Technology, Tehran, Iran

[2] Department of Materials Engineering , Malek Ashtar University of Technology, Esfahan. Iran

ARTICLE INFO

Article History:
Received 05 January 2021
Accepted 21 February 2021
Published 15 March 2021

Keywords:
Hybrid Nanocomposite
Nanoparticles
Titanium Dioxide
Copper
Phthalocyanine

ABSTRACT

Titanium dioxide-containing hybrid nanocomposites have been considered for their various applications in semiconductors, sensors, antibacterial and hygienic materials, photocatalysts, and solar cells. In this study, a new hybrid nanocomposite containing titanium dioxide nanoparticles modified with copper metal and the organic pigment phthalocyanine was successfully synthesized and characterized. For this purpose, first titanium dioxide nanoparticles modified with copper metal were prepared by the sol-gel method. Then, using the modified nanoparticles, a new hybrid nanocomposite was synthesized by the chemical precipitation method. Characterization of the modified nanoparticles and synthesized hybrid nanocomposites was conducted using X-ray diffraction (XRD) analysis, FT-IR spectroscopy, EDX analysis, reflection spectroscopy, concurrent thermal analysis (TG, DTA) and Abbott electron microscopy. Our results confirm the formation of a hybrid nanocomposite containing modified titanium dioxide nanoparticles and the organic pigment phthalocyanine with pure anatase phase. TEM micrograph showed a particle size of hybrid nanocomposite of about 20 nm. The band gap of the resulting hybrid nanocomposite was 2.80 eV, which was significantly reduced compared to the pure titanium dioxide (3.17 eV). As a result, the synthesized hybrid nanocomposite is very suitable for photocatalytic, photovoltaic and super hydrophilic applications under sunlight due to its absorption edge in the visible region.

How to cite this article
Gharagozlou M., Zhahabi S. Synthesis and Characterization of Novel Hybrid Nanocomposite containing Modified Titanium Dioxide Nanoparticles with Copper and Phthalocyanine Pigment. Nanochem Res, 2021; 6(1):94-103. DOI: 10.22036/ncr.2021.01.009

INTRODUCTION

Among the mineral oxides, titanium dioxide (TiO_2) is highly regarded due to its chemical stability, non-toxicity and low cost. The optical activity of titanium dioxide includes its photocatalytic, photovoltaic and super hydrophilic properties. The mechanism of action includes irradiating light with energy higher than the band gap energy of titanium dioxide and electron excitation from the valence level to the conduction level [1].

* Corresponding Author Email: *gharagozlou@icrc.ac.ir*

However, the use of titanium dioxide is limited for two reasons [2]:

1- The titanium dioxide band gap is in the UV region, while only 3% of the sunlight spectrum is in this domain.

2- Rapid electron-hole coupling and consequent loss of photocatalytic activity.

Therefore, in recent years, various methods have been used to modify the band gap energy and increase the optical activity of titanium dioxide, such as reducing the particle size, increasing the

specific surface area, and pairing titanium dioxide with other semiconductors. The modification of titanium dioxide with metals and non-metals and the sensitization of titanium dioxide has been mentioned previously [3].

There are many methods for depositing metal ions in TiO_2 semiconductors, but the two main methods used are as follows [4]:

1. Physical induction method performed by the bombardment of the semiconductor with a high-energy beam of metal ions.

2- Chemical modification method, which is mainly conducted through the sol-gel method. The Sol-gel method is one of the most widely used methods of preparing nanomaterials. In this method, combining the active metal in the cell allows the metal to interact directly with the preservative during the gelling step [5].

The optical activity of TiO_2 modified with metals is significantly dependent on the method of preparation, the nature of the ion and its concentration. Some researchers claim that metal modification reduces the energy thresholds of TiO_2. This produces two levels with a narrower energy difference, which leads to less energy consumption for the photocatalytic process. In addition, metals act as traps for electrons or holes preventing the electron–hole recombination. By increasing the lifespan of charge carriers, optical and photocatalytic activity may increase [8-6]. Various organic compounds such as safranin [7], eosin [8], rhodamine [9], thionine [10], macrocycles [12 and 11], etc. have been used as sensitizers for the sensitization of titanium dioxide.

The sensitizer is fixed on the surface of TiO_2 particles. Stabilization of sensitizing molecules on the semiconductor surface is done in different ways such as covalent bonding, ion pair bonding, physical adsorption, trapping in pores, and hydrophobic interaction [13]. Oxidation-reduction pairs are used to reproduce the sensitizing compound. If the process of reproducing the sensitizing compound is limited and prohibited, the sensitizing compound will undergo oxidative damage due to the attack of active radicals [4]. Phthalocyanine (Pc) is an organic pigment consisting of a 16-membered ring [14] in which the ring of carbon and nitrogen atoms is intertwined, and it is a combination of four isoindole molecules. The family of phthalocyanine organic pigments has high thermal and chemical stability and high intensity of light absorption in the visible region [15].

In this study, in order to overcome the aforementioned limitations of titanium dioxide and to correct its band gap, a new hybrid nanocomposite containing titanium dioxide nanoparticles modified with copper metal and phthalocyanine organic pigment was synthesized and identified. For this purpose, in the first stage, modified titanium dioxide nanoparticles were prepared by the sol-gel method. Then hybrid nanocomposite using modified titanium dioxide nanoparticles has been synthesized by the chemical deposition method using non-toxic, inexpensive and available materials. The advantages of these methods include the ease of the methods, production of high purity products, available raw materials and their reproducibility.

EXPERIMENTAL

Details of Precursors

Tetraisopropyl orthotitanate ($Ti(OC_3H_7)_4$, purity: 98%, molecular weight: 255.284 g/mol, density: 0.96 kg/L), copper nitrate (II) hydrate (purity: 99%), and ethanol (purity: 99.95%, molecular weight: 0.488 g/mol, density: 0.3789 g/cm^3) were purchased from Merck Co. Phthalocyanine ($C_{32}H_{18}N_8$, Purity: 99%, molecular weight: 514.54 g/mol) was purchased from ACROS Co.

Synthesis of undoped TiO_2 nanoparticles

TiO_2 nanoparticles were prepared by the sol-gel procedure [16]. 19 mL of $Ti(OC_3H_7)_4$ was slowly added to 20 mL ethanol under vigorous stirring for 1.5 h. The solution was subsequently left for several days to form a gel. The gel was dried at 100 °C for 6 h and then milled by a mortar. The obtained powder was calcined at 400 °C for 4 h at the rate of 2 °C/min.

Synthesis of Cu-TiO_2 nanoparticles

19 mL of $Ti(OC_3H_7)_4$ was gradually added to 20 mL ethanol under vigorous stirring (solution A). Then, 0.822 g of $Cu(NO_3)_2$ was dissolved in 5 mL of ethanol and added dropwise to solution A. After stirring for 1.5 h, the solution was left for several days to form a gel. The gel was dried at 100 °C for 6 h and then milled by a mortar. The obtained powder was calcined at 400 °C for 4 h at the rate of 2 °C/min.

Synthesis of Pc-Cu- TiO_2 hybrid nanoparticles

1 g of Cu-TiO_2 nanopowder was dispersed in 50

mL ethanol under ultrasonication for 60 min at 60 W. Then, 0.01 g of phthalocyanine was dissolved in 50 mL ethanol and added dropwise to the dispersant solution. The resulting solution was refluxed for 2 h at 70 °C. Subsequently, the formed nanocomposite was separated by high-speed centrifugation and dried at 70 °C for 1 h.

Characterization

A PerkinElmer FT-IR spectrophotometer was used to identify the functional groups in the precursors. For sample preparation of FT-IR, about 1/8 of the solid sample on a microspatula and about 0.25-0.50 teaspoons of KBr are taken. Then, they are mixed thoroughly in a mortar while grinding with the pestle. If the sample is in large crystals, the sample is grinded separately before adding KBr. A CE7000-A spectrophotometer was employed to determine the absorption edge. The morphology of the samples was assessed by scanning electron microscopy (Philips XL 40SEM). A Zeiss EM 900 transmission electron microscopy was used to characterize nanoparticles and nanocomposites. For sample preparation of TEM, a small drop of colloidal suspension (usually about 5 µl) is pipetted onto a TEM grid and simply allowed to dry at room temperature. The grid can then be directly observed in a TEM once the medium is evaporated. TG/DTA analysis (Perkin Elmer Pyris Diamond model) was performed at a scanning rate of 5o/ min. For sample preparation of TG/DTA, sample size should be between 2 and 50 mg. Many small pieces of sample are better than one large chunk. It is better to have a large surface area exposed to the sample purge. Crystalline structure of the samples was evaluated by a German-based Thermo-Noran X-ray diffraction analyzer. For sample preparation of XRD, nanopowders were prepared by hand grinding using a mortar and pestle. The mortar and pestle can be made out of a variety of materials such as agate, corundum, or mullite.

RESULTS AND DISCUSSION

Crystalline and Phase Structure

The X-ray diffraction patterns obtained from TiO_2, Cu-TiO_2, and Pc-Cu-TiO_2 H-NCs calcinated at different temperatures are shown in Fig. 1. Results show that anatase is the dominant phase in all the samples. However, the rutile primary peak at 2θ= 27.3° was also observed in Cu-TiO_2 sample

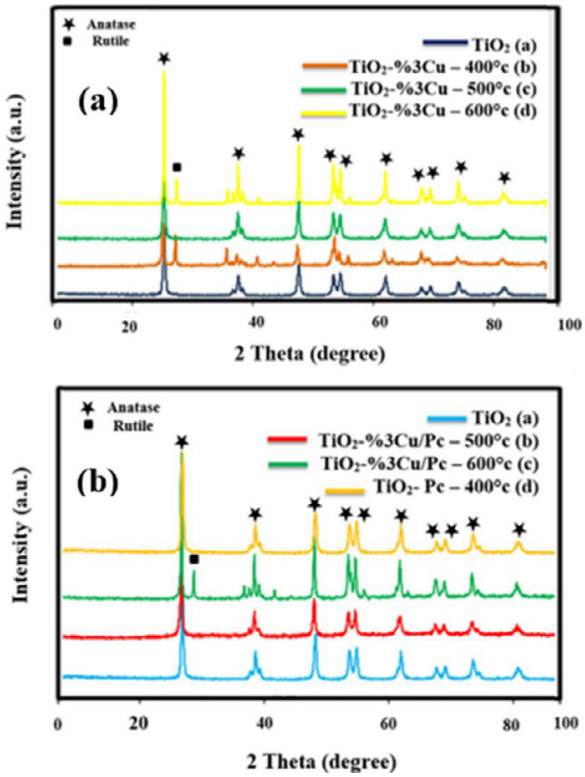

Fig. 1. X-ray diffraction patterns of: (a) Cu-TiO_2 and (b) Pc-Cu-TiO_2 H-NCs calcinated at different temperatures

Table 1. Crystallite size of samples calculated using the Scherer equation

Sample	Calcination temperature (°C)	Crystallite size (nm)
TiO_2	400	24.7
Cu-TiO_2	400	15.4
Cu-TiO_2	500	17.3
Cu-TiO_2	600	21.6
Pc-Cu-TiO_2	500	18.0
Pc-Cu-TiO_2	600	21.2

calcined at 400 °C and 600 °C, and, in Pc-Cu-TiO_2 H-NCs calcined at 600 °C [15]. Copper species are believed to leave the lattice in small quantities and form nanoclusters which cannot be detected by the XRD analysis [15].

In addition, taking the Hume-Rothery law and the ionic radii of copper (86.2 pm) and titanium (74.6 pm) into closer consideration, if the ionic radius difference is less than 15%, no new phase is formed [17]. Here, copper and titanium have nearly identical ionic radii. Hence, copper is most likely dissolved in the crystalline lattice of titania and does not form a new copper-based phase. The formation of copper solid solution in titania can be realized by comparing the X-ray diffraction patterns of the doped sample and pure titanium dioxide (Fig. 1a). As is seen, CuO peaks are visible at $2\theta = 35.6^{o}$ and $2\theta = 38.73^{o}$ [18], and as the calcination temperature increases, the peak intensity of copper oxide increases as well [19].

For the Pc-Cu-TiO_2 H-NCs sample calcined at 500 °C, the diffraction peaks of the anatase phase remained unchanged, indicating that the size and crystalline phase of the titania matrix did not change with the addition of phthalocyanine to the Cu-TiO_2 NPs. Peaks corresponding to the phthalocyanine have not been identified in XRD patterns, which may be due to the low concentration of Pc that is not detectable by XRD analysis [20]. The crystallite size of undoped TiO_2, Cu-TiO_2, and Pc-Cu-TiO_2 H-NCs at different calcination temperatures, calculated using the Scherer equation [20], are shown in Table 1.

The crystallite size of the samples was estimated from XRD peak broadening using the Scherrer equation [20].

$$t = 0.9\,\lambda / \beta \cos\theta$$

where t is the crystallite size, λ the wavelength of X-ray radiation (Cu$K\alpha$), θ the Bragg angle, and β the full width at half maximum (FWHM) of the most intense diffraction peak.

The crystallite size of the Cu-TiO_2 sample is smaller than that of Pc-Cu-TiO_2 H-NCs. The presence of copper in the titania matrix as a solid solution prevents the growth of TiO_2 crystals [27]. However, in the case of Pc-Cu-TiO_2 H-NCs, the addition of phthalocyanine results in the expansion of the titania lattice [27]. According to Table 1, the particle size also increased with increasing the calcination temperature.

Thermal Characteristics

TG/DTA curves of the precursors of the Cu-doped titanium dioxide and Pc-Cu-TiO_2 H-NC are shown in Figs. 2a and 2b, respectively. The endothermic peak at 100 °C is due to the water absorption and alcohol elimination that leads to a weight loss of 7.77% [21]. The two exothermic peaks at 180 °C and 220 °C are related to the decomposition of organic matters and the removal of -OH groups. The broad exothermic peak at 468 °C can be attributed to the burning of organic compounds through changing the amorphous phase to the anatase phase [22].

The volume reduction is about 32%, which is demonstrated in the TG curve over the temperature range of 100-500 °C. The anatase to rutile phase transformation takes place at temperatures between 450 and 800 °C. The transition temperature depends on the type of the precursor and the conditions of the nanoparticles preparation [23].

The TGA curve in Fig. 2b demonstrates three weight losses of 14%, 20%, and 36.9% at 98, 250, and 372 °C, respectively. The DTA curve shows an exothermic peak at temperatures between 310 and 400 °C, which corresponds to the formation of the anatase phase. It should be noted that the exothermic peak of the anatase generally occurs at 460 °C; however, the transformation has occurred below 460 °C due to the presence of copper [24].

The exothermic peaks in the range of 250 to 400 °C are attributed to the oxidation and burning of organic compounds in the gel [24]. The broad peak in the case of Pc-Cu-TiO_2 H-NC is attributed to the

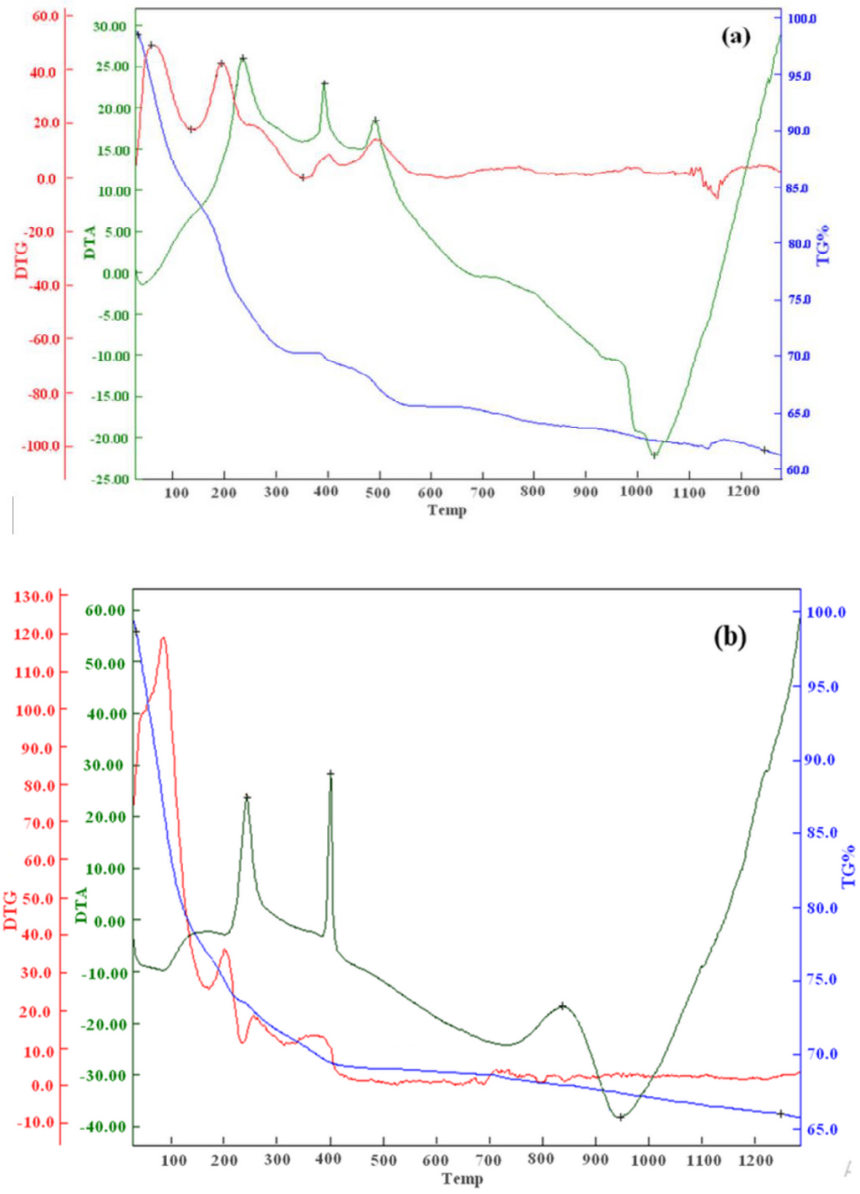

Fig. 2. Thermal behavior of precursors: (a) Cu-TiO_2 and (b) Pc-Cu-TiO_2 H-NC

crystallization of amorphous TiO_2 and the release of energy over this temperature range. Copper doping also decreased the anatase transformation temperature [24]. In general, exothermic peaks at low temperatures can be related to the decomposition and oxidation of acetate chelate, i.e. the cleavage of Ti-O bonds in $(TiO_2)_n$-O-CO-CH_3, while those at high temperatures can be due to the oxidation of the alkoxide, i.e. the cleavage of Ti-O bonds in $(TiO_2)_n$-O-C_4H_9 [25]. The peak at 510°C corresponds to the pyrolysis of the phthalocyanine [26].

Microstructural analysis

SEM images of Cu-TiO_2 and Pc-Cu-TiO_2 H-NC are presented in Fig. 3. The Cu-TiO_2 sample consists of a mixture of spherical and rod-shaped agglomerates (Fig. 3a). The Pc-Cu-TiO_2 nanocomposite shows a rod-like morphology (Fig. 3b), but the rod agglomeration degree and its aspect ratio (length to diameter) have increased.

TEM micrographs of Cu-TiO_2 and Pc-Cu-TiO_2 H-NC samples are shown in Fig. 4. The Cu-TiO_2 sample is composed of spherical particles with a diameter of 30 nm (Fig. 4a). Pc-Cu-TiO_2 H-NC

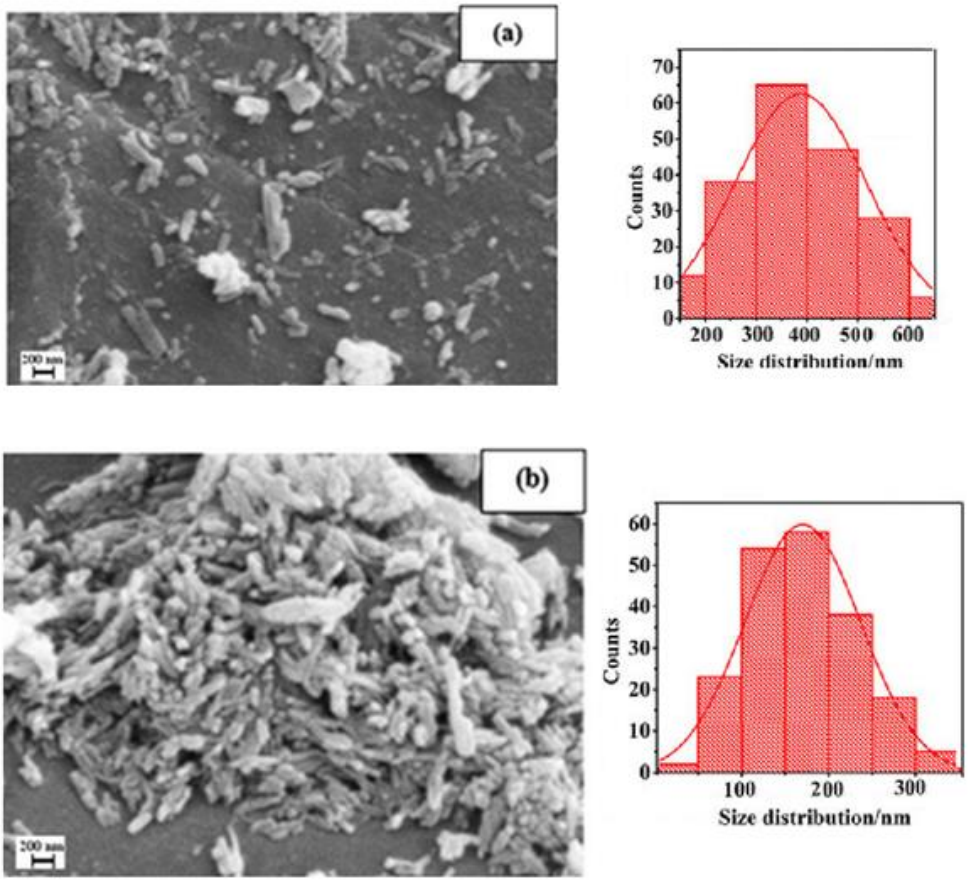

Fig. 3. SEM micrographs and histograms of: (a) Cu-TiO_2 and (b) Pc-Cu-TiO_2 H-NC

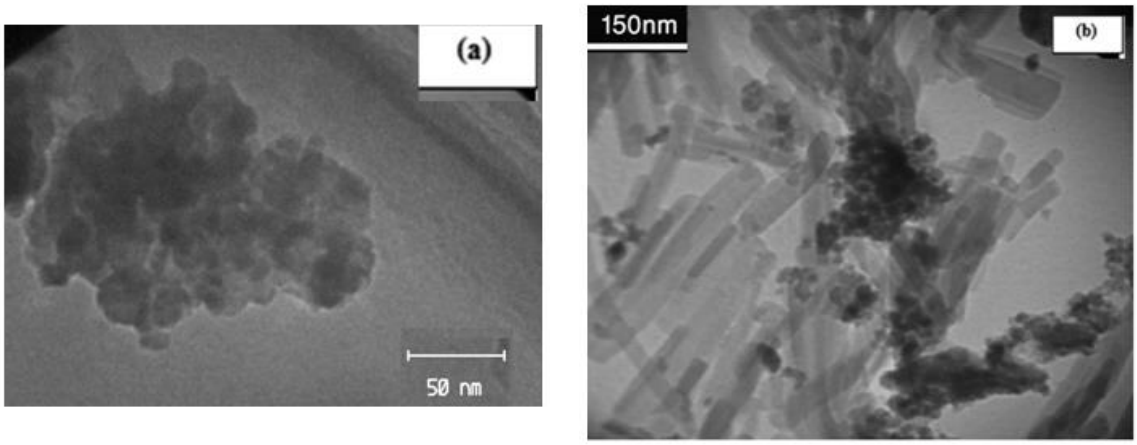

Fig. 4. TEM micrographs: (a) Cu-TiO_2 and (b) Pc-Cu-TiO_2 H-NC

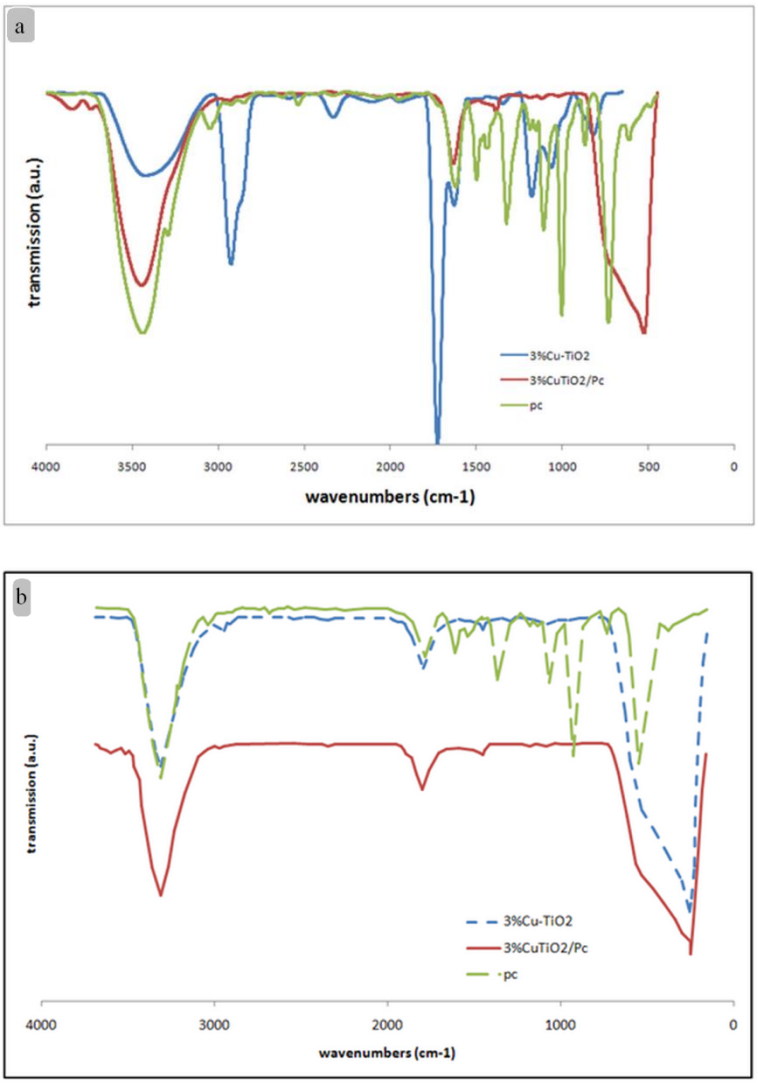

Fig. 5. IR results: (a) Cu-TiO_2, (b) Pc-Cu-TiO_2 H-NC, and (c) pure phthalocyanine.

sample is made of nanorods with a diameter of 25 nm and a length of 100 nm (Fig. 4b).

FT-IR analysis

The results of FTIR analysis of Cu-TiO_2 and Pc-Cu-TiO_2 H-NC samples are shown in Figs. 5a and 5b, respectively. The absorption peaks at 1628 cm^{-1} and 3431 cm^{-1} are attributed to the bending and stretching vibrations of O-H, respectively [27]. The adsorption peak at 1384 cm^{-1} for Cu-TiO_2 and Pc-Cu- TiO_2 H-NC may be related to the formation of copper oxide during calcination. Nitrate groups are removed during the calcination process, so this absorption cannot be due to the presence of nitrate groups. The small absorption band at 2390 cm^{-1} is related to the CO_2 from the atmosphere [28]. The absorption bands in the range of 900 to 400 cm^{-1} are attributed to Ti-O stretching vibration [29]. The absorption peak at 3860 cm^{-1} is due to the chemisorbed vibrations of water [14]. Fig. 5c shows the results of FTIR of the phthalocyanine sample. The absorption peaks in the range of 1600 to 1300 cm^{-1} are related to the stretching and bending vibrations of the phthalocyanine ligands [30]. The absorption peaks at 1495, 1443, and 1326 cm^{-1} are due to the C=C and C=N skeletal vibrations of the porphyrin rings, while other bands are attributed to CH deformation as well as C=C stretching and bending modes in the pyrrole ring [31].

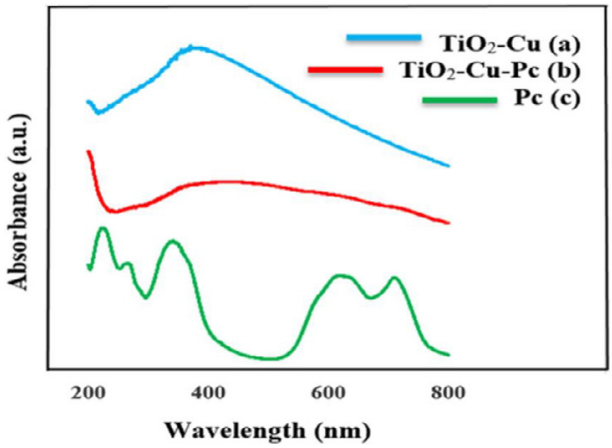

Fig. 6. The UV-visible spectroscopy data of: (a) Cu- TiO_2, (b) Pc-Cu- TiO_2 H-NC, and (c) pure phthalocyanine

Optical Properties

UV-visible spectroscopy curves for Cu-TiO_2, Pc-Cu-TiO_2 H-NC, and phthalocyanine are shown in Fig. 6. The results show that Cu-TiO_2 nanoparticles are capable of absorbing light at longer wavelengths and have a broader absorption spectrum in comparison to pure titanium dioxide. The adsorption edge of the Pc-Cu-TiO_2 H-NC is significantly shifted to the visible region, which is higher than that of the pure Cu- TiO_2 and TiO_2 NPs. The UV-Vis absorption spectroscopy for phthalocyanine shows π-π electron transfer of the aromatic ring and orbitals linked to the central atom of the metal [32].

The pristine TiO_2 at anatase phase shows an intense absorption in the UV region(around 350 nm). While the Cu-doped sample indicated a red shift extending up to 600 nm. This is attributed to the characteristic surface plasmon resonance of Cu nanoparticles. The successful doping of Cu is also evident from the change in the color observed in the samples, shifting from pure white to light yellow. The band gap values of pristine TiO_2 at anatase and rutile phases were observed to be 3.17 and 3.03 eV, respectively. The Cu-doped sample showed a significant dip in the band gap value up to 2.8 eV. The Tauc method was used to calculate the band gap of the samples [30].

Fig. 6 (c) shows an absorption in the UV region known as the Soret band (B), which is composed of three absorption peaks and two shoulders. A broad absorption band is located in the ultraviolet region before the UV absorption of the phthalocyanine molecule. Other well-known bands of the phthalocyanine molecule are the Q-band that appears in the 550–570 nm range. The high-energy Q-band peak shows the first π-π transition and the low-energy Q-band peak represents the second π-π transition of phthalocyanine. In the energetic region of the Soret band, which is close to 288 nm, there are many differences (could not understand) in the absorption spectrum of phthalocyanine. It can be attributed to the presence of a "d- band" attached to the central metal atom [33].

CONCLUSIONS

The hybrid nanocompound of phthalocyanine-copper-titania (Pc-Cu-TiO_2 H-NC) was synthesized by the sol-gel method. Their phase structure, morphology, thermal and optical properties were studied and compared to those of pure and copper-doped titania. It was found that Cu formed a solid solution in titania while Pc-Cu-TiO_2 formed an alloy. The anatase-rutile phase transformation was shown to be dependent upon the calcination temperature and the addition of dopants or alloying elements. A rod-like morphology with a particle size of 15-20 nm and different agglomeration tendency in Cu-TiO_2 and Pc-Cu-TiO_2 samples was illustrated. A red-shift in the absorption edge was observed in Pc-Cu-TiO_2 sample as compared to pure TiO_2 nanoparticles.

ACKNOWLEDGMENTS

Authors acknowledge the support by the Institute for Color Science and Technology.

CONFLICTS OF INTEREST

The authors announce that there are no conflicts of interest.

REFERENCES

1. R. Salehi, F. Dadashian, E. Ekrami, Acid Dyes Removal from textile wastewater using waste cotton activated carbon: Kinetic, isotherm, and thermodynamic studies, Progress in Color, Colorants and Coatings, 11 (2018) 9-20.
2. D. Mukesh, A. Kumar, Biotreatment of industrial effluents, in, Oxford: Elsevier, 2005.
3. Chan SHS, Yeong Wu T, Juan JC, Teh CY. Recent developments of metal oxide semiconductors as photocatalysts in advanced oxidation processes (AOPs) for treatment of dye waste-water. Journal of Chemical Technology & Biotechnology. 2011;86(9):1130-58.
4. M. Hosseini-Zori, Z. Mokhtari shourijeh, Synthesis, Characterization and Investigation of Photocatalytic Activity of transition metal-doped TiO_2 Nanostructures, Progress in Color, Colorants and Coatings, 11 (2018) 209-220.
5. Boikanyo D, Mishra SB, Ray S, Mhlanga SD, Mishra AK. Structure–Activity Relationships of Er3+ and MWCNT-Modified TiO2: Enhancing the Textural and Optoelectronic Properties of TiO2. The Journal of Physical Chemistry C. 2019;123(51):31246-61.
6. Chatterjee D, Dasgupta S. Visible light induced photocatalytic degradation of organic pollutants. Journal of Photochemistry and Photobiology C: Photochemistry Reviews. 2005;6(2-3):186-205.
7. Nishikiori H, Sato T, Kubota S, Tanaka N, Shimizu Y, Fujii T. Preparation of Cu-doped TiO2 via refluxing of alkoxide solution and its photocatalytic properties. Research on Chemical Intermediates. 2011;38(2):595-613.
8. Colón G, Maicu M, Hidalgo MC, Navío JA. Cu-doped TiO2 systems with improved photocatalytic activity. Applied Catalysis B: Environmental. 2006;67(1-2):41-51.
9. Sun S, Bao J, Gao C, Ding J. Photocatalytic degradation of gaseous o-xylene over M-TiO2 (M=Ag, Fe, Cu, Co) in different humidity levels under visible-light irradiation: activity and kinetic study. Rare Metals. 2011;30(S1):147-52.
10. Irie H, Miura S, Kamiya K, Hashimoto K. Efficient visible light-sensitive photocatalysts: Grafting Cu(II) ions onto TiO2 and WO3 photocatalysts. Chemical Physics Letters. 2008;457(1-3):202-5.
11. Ahmed SA. Structural, optical, and magnetic properties of Cu-doped TiO2samples. Crystal Research and Technology. 2017;52(3):1600335.
12. Seoudi R, El-Bahy GS, El Sayed ZA. Ultraviolet and visible spectroscopic studies of phthalocyanine and its complexes thin films. Optical Materials. 2006;29(2-3):304-12.
13. Iliev V, Tomova D. Photocatalytic oxidation of sulfide ion catalyzed by phthalocyanine modified titania. Catalysis Communications. 2002;3(7):287-92.
14. Lalitha K, Sadanandam G, Kumari VD, Subrahmanyam M, Sreedhar B, Hebalkar NY. Highly Stabilized and Finely Dispersed Cu2O/TiO2: A Promising Visible Sensitive Photocatalyst for Continuous Production of Hydrogen from Glycerol:Water Mixtures. The Journal of Physical Chemistry C. 2010;114(50):22181-9.
15. Byrne C, Fagan R, Hinder S, McCormack DE, Pillai SC. New approach of modifying the anatase to rutile transition temperature in TiO2 photocatalysts. RSC Advances. 2016;6(97):95232-8.
16. Mesgari Z, Gharagozlou M, Khosravi A, Gharanjig K. Spectrophotometric studies of visible light induced photocatalytic degradation of methyl orange using phthalocyanine-modified Fe-doped TiO2 nanocrystals. Spectrochimica Acta Part A: Molecular and Biomolecular Spectroscopy. 2012;92:148-53.
17. Bensouici F, Bououdina M, Dakhel AA, Tala-Ighil R, Tounane M, Iratni A, et al. Optical, structural and photocatalysis properties of Cu-doped TiO 2 thin films. Applied Surface Science. 2017;395:110-6.
18. Choi H, Kang M. Hydrogen production from methanol/water decomposition in a liquid photosystem using the anatase structure of Cu loaded TiO2TiO2. International Journal of Hydrogen Energy. 2007;32(16):3841-8.
19. Pintar A, Batista J, Hočevar S. TPR, TPO, and TPD examinations of Cu0.15Ce0.85O2−y mixed oxides prepared by co-precipitation, by the sol–gel peroxide route, and by citric acid-assisted synthesis. Journal of Colloid and Interface Science. 2005;285(1):218-31.
20. Wu N. Enhanced TiO2 photocatalysis by Cu in hydrogen production from aqueous methanol solution. International Journal of Hydrogen Energy. 2004;29(15):1601-5.
21. Arora N, Joshi DP. Band gap dependence of semiconducting nano-wires on cross-sectional shape and size. Indian Journal of Physics. 2017;91(12):1493-501.
22. A. Cenovar, P. Paunovic, A. Grozdanov, P. Makreski, E. Fidanccevska, Preparation of nano-crystalline TiO2 by Sol-gel method using titanium tetraisopropoxide (TTIP) as a precursor, Advances in Natural Science: Theory & Applications, (2012).
23. Crişan M, Brăileanu A, Răileanu M, Zaharescu M, Crişan D, Drăgan N, et al. Sol–gel S-doped TiO2 materials for environmental protection. Journal of Non-Crystalline Solids. 2008;354(2-9):705-11.
24. M.S. Lee, G.-D. Lee, S.S. Park, S.-S. Hong, Synthesis of TiO2 nanoparticles in reverse microemulsion and their photocatalytic activity, Journal of Industrial and Engineering Chemistry, 9 (2003) 89-95.
25. Martínez Vargas DX, Rivera De la Rosa J, Lucio-Ortiz CJ, Hernández-Ramirez A, Flores-Escamilla GA, Garcia CD. Photocatalytic degradation of trichloroethylene in a continuous annular reactor using Cu-doped TiO2 catalysts by sol–gel synthesis. Applied Catalysis B: Environmental. 2015;179:249-61.
26. Seoudi R, El-Bahy GS, El Sayed ZA. FTIR, TGA and DC electrical conductivity studies of phthalocyanine and its complexes. Journal of Molecular Structure. 2005;753(1-3):119-26.
27. Li Z, Hou B, Xu Y, Wu D, Sun Y, Hu W, et al. Comparative study of sol–gel-hydrothermal and sol–gel synthesis of titania–silica composite nanoparticles. Journal of Solid State Chemistry. 2005;178(5):1395-405.
28. Baneshi J, Haghighi M, Jodeiri N, Abdollahifar M, Ajamein H. Homogeneous precipitation synthesis of CuO–ZrO 2 –CeO 2 –Al 2 O 3 nanocatalyst used in hydrogen production via methanol steam reforming for fuel cell applications. Energy Conversion and Management. 2014;87:928-37.
29. Yan X, He J, G. Evans D, Duan X, Zhu Y. Preparation, characterization and photocatalytic activity of Si-doped and rare earth-doped TiO2 from mesoporous precursors. Applied Catalysis B: Environmental. 2005;55(4):243-52.
30. Farag AAM. Optical absorption studies of copper phthalocyanine thin films. Optics & Laser Technology. 2007;39(4):728-32.
31. Oshio H, Ama T, Watanabe T, Kincaid J, Nakamoto K. Structure sensitive bands in the vibrational spectra of metal complexes of tetraphenylporphine. Spectrochimica Acta Part A:

Molecular Spectroscopy. 1984;40(9):863-70.
32. G. Kumar, J. Thomas, N. George, B. Kumar, P. Radhakrishnan, V. Nampoori, C. Vallabhan, N. Unnikrishnan, Optical absorption studies of free (H_2Pc) and rare earth (RePc) phthalocyanine doped borate glasses, Physics and chemistry of glasses, 41 (2000) 89-93.
33. Hamam KJ, Alomari MI. A study of the optical band gap of zinc phthalocyanine nanoparticles using UV–Vis spectroscopy and DFT function. Applied Nanoscience. 2017;7(5):261-8.